Geophysical Journal International

*Geophys. J. Int.* (2016) **207,** 889–900
Advance Access publication 2016 August 15
GJI Geomagnetism, rock magnetism and palaeomagnetism

doi: 10.1093/gji/ggw243

# Rock magnetic investigation of loess deposits in the Eastern Qingling Mountains (central China) and its implications for the environment of early humans

Xiaoyong Wang,[1] Huayu Lu,[1] Weiguo Zhang,[2] Pengxiang Hu,[3] Hongyan Zhang,[1] Zhiyong Han,[1] Shejiang Wang[4] and Baoguo Li[5]

[1]*School of Geographic and Oceanographic Sciences, Nanjing University; Jiangsu Collaborative Innovation Center for Climate Change, Nanjing* 210023, *China. E-mail: wangxy@nju.edu.cn*
[2]*State Key Laboratory of Estuarine and Coastal Research, East China Normal University, Shanghai* 200062, *China*
[3]*Division of Tethys Research Center, Institute of Geology and Geophysics, Chinese Academy of Sciences, Beijing* 100029, *China*
[4]*Institute of Vertebrate Paleontology and Paleoanthropology, Chinese Academy of Sciences, Beijing* 100044, *China*
[5]*Ministry of Education Laboratory for Plant–Soil Interaction Processes, College of Natural Resources and Envir. Science, China Agricultural University, Beijing* 100094, *China*

Accepted 2016 June 23. Received 2016 June 21; in original form 2016 March 3

## SUMMARY

The Luonan Basin, located in the transitional zone between temperate and subtropical China, is an important locality for human evolution during the early to middle Pleistocene. The loess deposits in the Luonan Basin contain numerous *in situ* lithic artefacts; the deposits also constitute suitable material for dating the artefacts and are potentially useful for reconstructing the climatic fluctuations which is important for studying the adaptation and occupation of the area by early humans. We carried out a combined rock magnetic and geochemical investigation of a loess sequence from the Liuwan Palaeolithic site in the Luonan Basin. The results indicate a mixture of magnetic minerals, including magnetite/maghemite and hematite/goethite. Magnetic susceptibility was used as a palaeoclimate proxy on the Chinese Loess Plateau; however, its application to the Luonan Basin may be problematic because the provenance of the loess parent material, as well as the depositional environment, differs from that of the Chinese Loess Plateau. We found that rock magnetic parameters related to the grain size of magnetic minerals, such as SIRM/$\chi$ and $\chi_{ARM}$/SIRM, are better palaeoclimatic indicators than magnetic susceptibility. Overall, the magnetic results, together with the results of bulk grain-size and chemical index of alteration, indicate that the interglacial environment of early humans in Luonan Basin was warmer and more humid than the coeval environment of the Chinese Loess Plateau.

**Key words:** Environmental magnetism; Rock and mineral magnetism; Asia.

## 1 INTRODUCTION

The Luonan Basin is an intermontane depression located in the Qinling Mountains, central China. The series of mountains to the north are approximately 2000 m (ABSL) high, and those to the south range in elevation from 1300 to 1700 m (ABSL) (Fig. 1). Over 10 000 lithic artefacts, including those from the surface as well as *in situ*, have been excavated from the basin (Wang 2005; Wang *et al*. 2005; Lu *et al*. 2011a). These findings indicate that the Luonan Basin was an important area for hominin settlement in the Old World after the initial expansion of early humans out of Africa (Zhu *et al*. 2003; Norton & Bae 2008). Palaeomagnetic and optically stimulated luminescence studies of the loess deposits, which contain *in situ* stone tools in different layers, indicate that hominins occupied this region repeatedly from 0.8–0.7 to 0.4–0.3 and from ~0.2 to 0.1 Ma (Lu *et al*. 2007, 2011b). The loess deposits in the Luonan Basin not only provide suitable material for dating lithic artefacts but are also potentially useful for reconstructing the climatic fluctuations which constitute an essential background for studying the adaptation and occupation of the area by early humans. However, although many palaeoclimatic records have been obtained from the Chinese Loess Plateau (CLP) located to the north of the Qinling Mountains, the palaeoenvironment of the Palaeolithic sites in the Luonan Basin remains poorly resolved.

Magnetic measurements have been used successfully for reconstructing the climatic and environmental evolution of the thick loess deposits of the CLP, which are regarded as one of the best environmental archives for the past 2.5 Ma (Heller & Liu

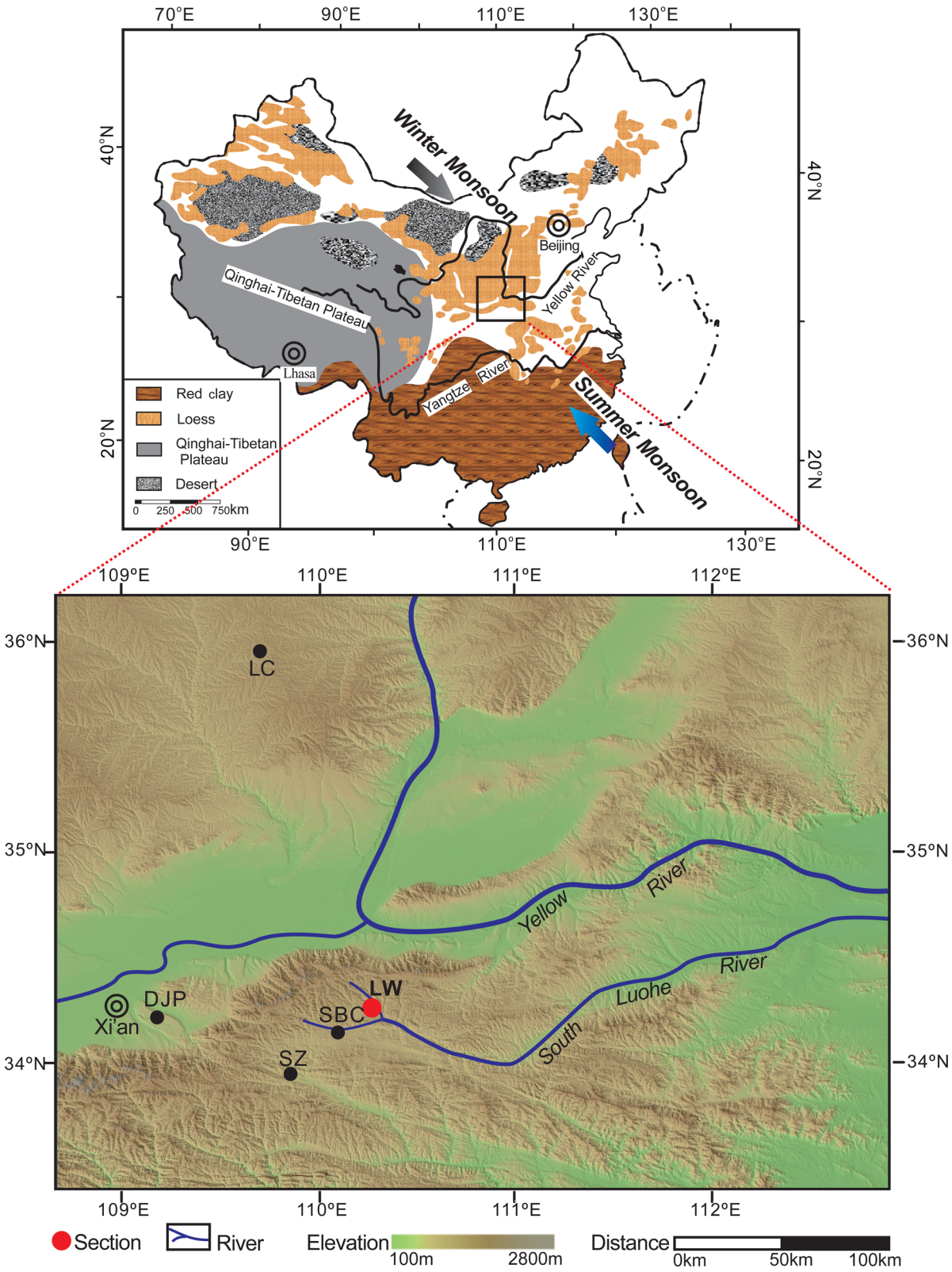


**Figure 1.** Major geographical regions of China, the distribution of loess deposits, directions of the summer and winter monsoons, and sites referenced in the text (LW: Liuwan) and mentioned (LC: Luochuan; DJP: Duanjiapo; SBC: Shangbaichuan; SZ: Shangzhou).

1982; Kukla *et al*. 1988; An 2000). On the CLP, the warm and humid interglacial periods produced magnetically enhanced fossil soils (palaeosols), characterized by higher values of magnetic susceptibility, which are intercalated with less intensively weathered and more weakly magnetic loess layers corresponding to cold, dry glacial periods. The fluctuations of the magnetic susceptibility of the loess-palaeosol sequences on the CLP have been shown to co-vary significantly with the waxing and

**Table 1.** Description for the stratigraphic units of the Liuwan section.

| Description | Interpretation |
|---|---|
| 0.5–1.3 m: light brown (7.5YR 5/6), abundant worm and insect burrows, transitional upper and lower boundaries | Loess ($L_I$) |
| 1.3–2.4 m: dull reddish brown (5YR 4/4), granular, occasional ferromanganese mottles and black charcoal. | Palaeosol ($S_I$) |
| 2.4–2.8 m: light brown (7.5YR 5/6), occasional carbonate nodules (Ø 0–5 mm), sharp lower and upper boundaries | Loess ($L_{II}$) |
| 2.8–3.6 m: dull reddish brown (5YR 4/4), granular, occasional ferromanganese mottles | Palaeosol ($S_{II}$) |
| 3.6–4.0 m: light yellowish brown (10YR 6/6), occasional ferromanganese mottles, sharp lower and upper boundaries | Loess ($L_{III}$) |
| 4.0–5.8 m: reddish brown (5YR 4/6), granular, occasional ferromanganese cutans, occasional irregular greyish yellow (5Y 6/4) aggregates | Palaeosol ($S_{III}$) with weakly gleyzation at the base |
| 5.8–6.0 m: light yellowish brown (10YR 6/6), little olive yellow (5GY 8/3) aggregates, sharp upper boundary and gradual lower boundary | Weakly gleyic loess ($L_{IV}$) |
| 6.0–7.0 m: dull reddish brown (5YR 4/4), granular, occasional greyish yellow (5Y 6/4) aggregates and ferromanganese cutans | Weakly gleyic palaeosol ($S_{IV}$) |
| 7.0–7.4 m: light brown (7.5YR 5/6), occasional irregular olive yellow (5GY 8/3) aggregates (Ø 0–3 cm) and numerous ferromanganese mottles, transitional upper and lower boundaries | Gleyic loess ($L_V$) |
| 7.4–8.2 m: reddish brown (5YR 4/6), granular, occasional irregular olive yellow (5GY 8/3) aggregates (Ø 0–3 cm), numerous ferromanganese mottles | Gleyic palaeosol ($S_V$) |
| 8.2–9.4 m: light brown (7.5YR 5/6), numerous irregular olive yellow (5GY 8/3) aggregates (Ø 0–3 cm) and ferromanganese mottles and cutans, especially at the base, transitional upper and lower boundaries | Gleyic loess ($L_{VI}$) |
| 9.4–9.9 m: reddish brown (5YR 4/6), granular, occasional irregular olive yellow (5GY 8/3) aggregates (Ø 0–3 cm)and black ferromanganese cutans | Gleyic palaeosol ($S_{VI}$) |
| 9.9–11.8 m: light brown (5YR 4/6), numerous irregular olive yellow (5GY 8/3) aggregates (Ø 0–3 cm) and ferromanganese cutans, transitional upper boundary and sharp lower boundary with the underlain poorly sorted alluvial gravel layer. | Gleyic loess ($L_{VII}$) |

waning of the East Asian monsoon circulation (An 2000; Maher & Hu 2006).

Loess deposits in South China, designated the Xiashu Loess, are mainly distributed in the middle and lower reaches of the Yangtze River. The Xiashu Loess is also characterized by clear loess-palaeosol alternations (Li & Yang 1999; Zheng 1999; Qiao *et al*. 2003; Zhang *et al*. 2007); however, the deposits exhibit a more complex linkage between magnetic parameters (e.g. magnetic susceptibility) and palaeoclimate. Zhang *et al*. (2007) suggested that the magnetic susceptibility record of the Xiashu loess does not clearly reflect pedogenic intensity. In addition, Hu *et al*. (2009) suggested that the magnetic susceptibility record of eolian deposits in subtropical China are significantly affected by post-depositional hydromorphic processes, and thus can't be used to reconstruct palaeoclimatic variations.

The Luonan Basin is located at the geographical boundary between temperate and subtropical China and therefore the loess deposits of the region potentially have different magnetic properties to those both of the CLP and South China. The nature of any linkages between loess magnetic properties and the climate of the region is unknown. Here, we present the results of a combined magnetic and geochemical investigation of a loess-palaeosol profile in the Luonan Basin, designated the Liuwan section, in order to assess possible magnetic-palaeoclimate linkages and to assess their implications for early human occupation.

## 2 GEOLOGICAL SETTING AND SAMPLING

The Luonan Basin is located in a region with a warm, semi-humid climate. The mean annual temperature is 11.1 °C and the mean annual precipitation is 754.8 mm. The South Luohe River and the Danjiang River are the main river systems in the area (Fig. 1). Loess deposits, with a thickness ranging from 2 to 25 m, are mainly distributed on the river terraces, or mantled on the flat piedmont slopes (Zhang *et al*. 2012). Using a combination of pedostratigraphy, magnetostratigraphy and optically stimulated luminescence (OSL) dating, Lu *et al*. (2007, 2011a) established a chronological framework for the loess-palaeosol sequences in the area and suggested that the loess started accumulating at least 1.1 Ma.

The Liuwan loess profile (38°08′37′ N, 110°08′13′ E, 948 m ABSL) lies on the terrace of South Luohe river and is regularly excavated for clay by brick factory workers. More than hundred artefacts discarded on the quarry floor during clay removal, and about hundred *in situ* artefacts have been identified in different layers (Shaanxi Provincial Institute of Archaeology Cultural Relics Administrative Committee of Shangluo District 2007; Lu *et al*. 2007, 2011b). Field investigations indicated that the studied profile is representative in the Luonan Basin.

The base of the investigated profile is an alluvial layer (11.8–13 m) characterized by poorly sorted sand and gravel, and the top (0–0.5 m) consists of reworked modern soil. The central 11.3-m-thick (0.5–11.8 m) section, containing 13 units recognized on the basis of lithological and pedological characteristics (Table 1), can be further divided into two subsequences (Fig. 2): (1) Subsequence I (0.5–7.0 m) is characterized by relatively thicker palaeosol layers with respect to loess layers and clear loess-palaeosol boundaries. It comprises 4 loess layers ($L_I$, $L_{II}$, $L_{III}$, $L_{IV}$) and 4 palaeosol layers ($S_I$, $S_{II}$, $S_{III}$, $S_{IV}$), and weakly gleyic feature are present in the lower part of this subsequence (the base of $S_{III}$, $L_{IV}$, $S_{IV}$). (2) Subsequence II (7.0–11.8 m) is characterized by a transitional boundary and hydromorphic properties and consists of 3 loess layers ($L_V$, $L_{VI}$, $L_{VII}$) and 2 intervening palaeosols ($S_V$, $S_{VI}$). Previous OSL dating has provided an age control for the Liuwan loess-palaeosol sequence. OSL dates for the depths of 80, 140, 320 and 420 cm are 146.4 ± 12.3, 137.0 ± 13.4, 151.6 ± 4.9 and 202.2 ± 6.9 ka, respectively (Lu *et al*. 2007). Based on their stratigraphic position and the OSL chronology, we assume that the magnetic susceptibility peaks in subsequence I of the Liuwan section correspond to palaeosols S1–S5 of the standard Luochuan loess-palaeosol sequence on the CLP (Fig. 3). However, the clarity of the magnetic susceptibility stratigraphy is affected by welding and pedogenic overprinting because of the lower sedimentation rate and intensive pedogenesis. A total

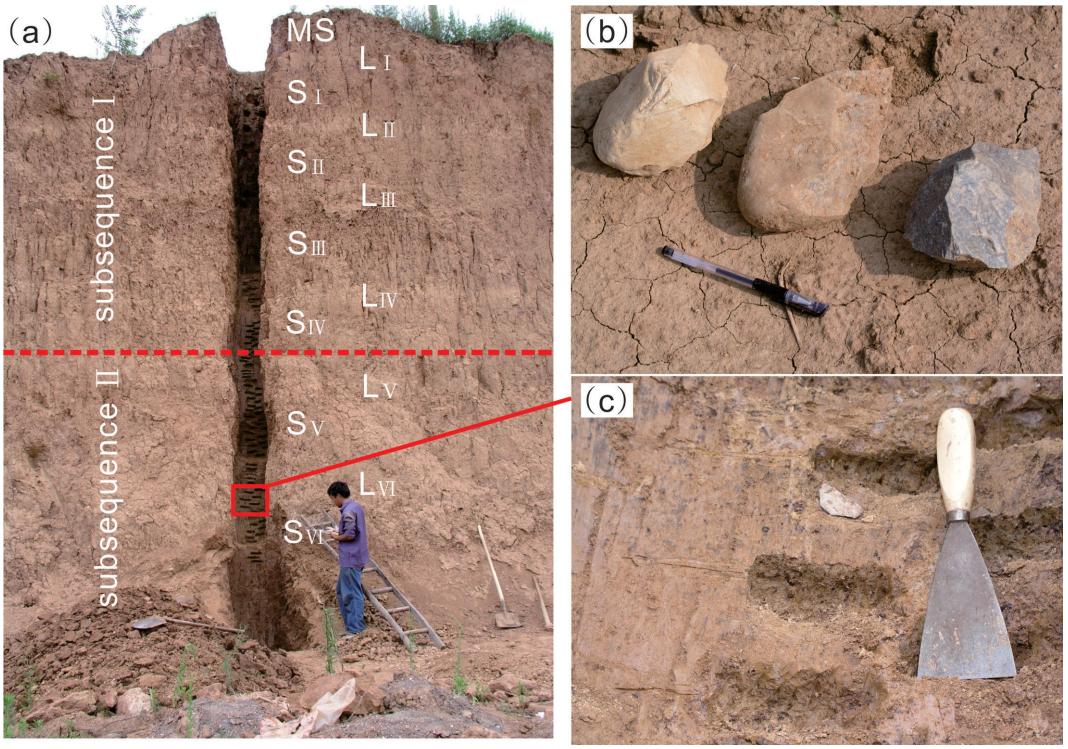


**Figure 2.** Liuwan loess section (a), lithic artefacts from the loess deposits (b) and irregular olive yellow aggregates, ferromanganese mottles and cutans in subsequence II (c).

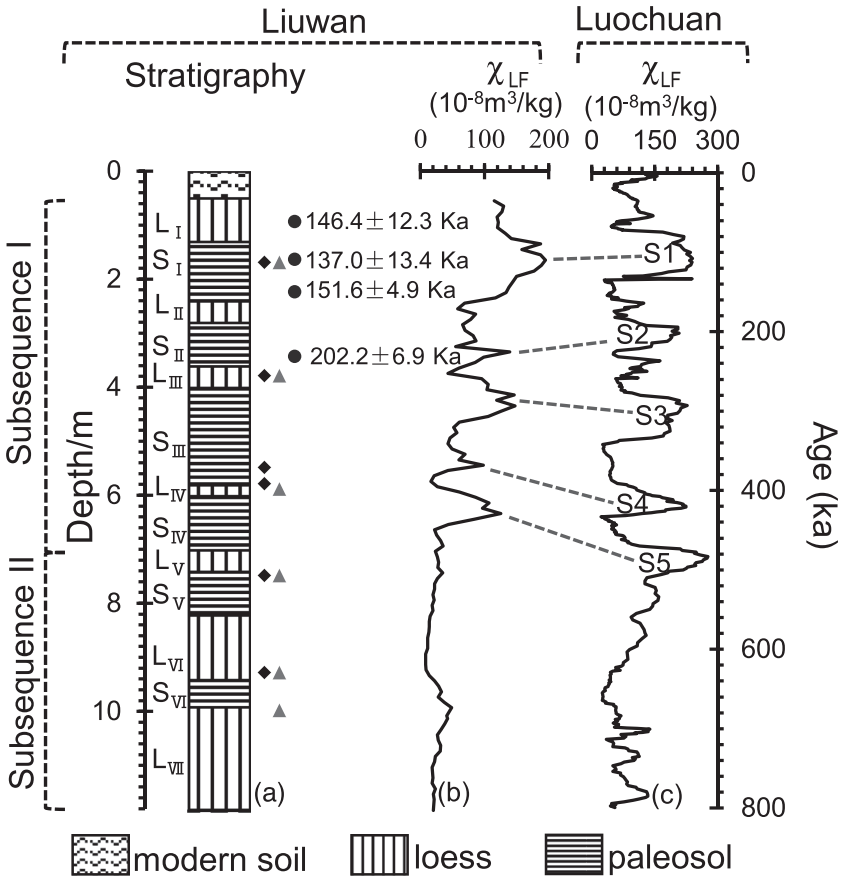


**Figure 3.** Pedostratigraphy (a), magnetic susceptibility (b) and their comparison with the Luochuan loess sequence (c) in the central Chinese Loess Plateau (Bloemendal & Liu 2005). Solid diamonds, triangles and circles are the locations of samples collected for high-temperature magnetic susceptibility and hysteresis loop measurements and OSL analyses.

of 113 samples at a 10-cm-interval from the central 11.3-m-thick section were used in this study.

## 3 METHODS

### 3.1 Magnetic measurements

The samples were oven-dried at a temperature of 40 °C and then gently disaggregated by hand and placed into weakly magnetic plastic boxes of 10.8 $cm^3$ volume. Sample masses ranged between 7.9 and 8.1 g. Mass-specific magnetic susceptibility was determined using an MS2 Bartington susceptibility meter with a B sensor at frequencies of 470 Hz ($\chi_{LF}$) and 4700 Hz ($\chi_{HF}$). Frequency-dependent magnetic susceptibility ($\chi_{FD}$) was calculated as $\chi_{LF}$-$\chi_{HF}$. The high-temperature magnetic susceptibility, between room temperature and 700 °C ($\chi$-T), of selected samples was measured using a KLY-3 Kappabridge with a CS-3 high-temperature furnace (Agico Ltd. Brno) in an argon atmosphere.

ARM was imparted in a 0.05 mT DC field superimposed on a peak AF (alternating field) demagnetizing field of 100 mT using a DTECH 2000 AF demagnetizer, and is expressed as susceptibility of ARM ($\chi_{ARM}$). Isothermal remanent magnetization (IRM) was imparted in a 1 T DC field, followed by the application of a backfield of 300 mT; hereafter these measurements are termed SIRM and $IRM_{-300\,mT}$, respectively. An S-ratio was calculated from the backfield data as: $S_{-ratio} = -IRM_{-300mT}/SIRM$, and 'hard' isothermal remanent magnetization (HIRM) was calculated as: $HIRM = 0.5 \times (SIRM + IRM_{-300\,mT})$ (Robinson 1986; Bloemendal *et al*. 1992). Hysteresis parameters of selected samples were measured using a Variable Field Translational Balance (VFTB) with a maximum field of ±1 T. Saturation magnetization ($M_s$), saturation remanence ($M_{rs}$) and coercivity ($B_c$) were determined after correction for the paramagnetic contribution identified from the slope of the magnetization curve at high fields. Subsequently, coercivity of remanence ($B_{cr}$) was obtained by SIRM demagnetization using the VFTB.

### 3.2 Geochemical and particle-size measurements

After eolian dust is deposited, varying degrees of decalcification during pedogenesis can cause the calcium carbonate content to vary significantly with depth. Carbonate was removed by grinding the samples with an agate mortar, followed by acid leaching using 1 mol $L^{-1}$ acetic acid (HAc). This allowed to eliminate the influence of variations in carbonate concentrate on element concentrations (Liang *et al*. 2009; Yang *et al*. 2009). The concentrations of major elements were measured using an X-ray fluorescence spectrometer (XRF-1800). The chemical index of alteration (CIA) was calculated as $CIA = [Al_2O_3/(Al_2O_3 + CaO^* + Na_2O + K_2O)] \times 100$ (molar ratio), where $CaO^*$ represents the amount of CaO in the silicate fraction of the sample (Nesbitt & Young 1982).

The particle grain size was measured using a Malvern Mastersizer 2000 after pretreatment with hydrogen peroxide ($H_2O_2$) to remove organic matter, with hydrochloric acid (HCl) to remove carbonates and finally with sodium hexametaphosphate ($(NaPO_3)_6$) to facilitate dispersion (Lu & An 1998).

## 4 RESULTS

### 4.1 Magnetic mineralogy

Magnetic mineral assemblages and their variation within loess-palaeosol sequences can provide palaeoclimatic information. The measurement of the variation of magnetic susceptibility between

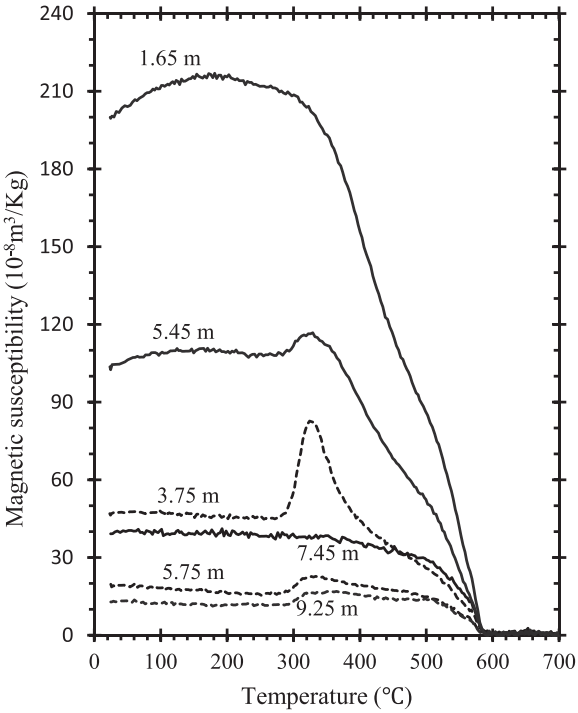


**Figure 4.** Results of high-temperature magnetic susceptibility measurements ($\chi$-T heating curves) of selected samples from the Liuwan section.

room-temperature and 700 °C ($\chi$-T) can provide information about magnetic mineralogy by observation of Curie temperatures, transition temperatures and mineralogical changes during thermal treatment (Dunlop & Özdemir 1997; Liu *et al*. 2005). Typical plots of $\chi$-T of samples from the Liuwan section are shown in Fig. 4. A significant increase in magnetic susceptibility after thermal treatment (not shown here) was observed for all samples and may resulted from the neo-formation of strongly magnetic phases of Fe-bearing aeolian minerals (Hunt *et al*. 1995). A steady increase of susceptibility below ~200 °C, due to the temperature dependence of single domain particles, is observed for samples from 1.65 and 5.45 m, but not in the case of samples from 5.75, 7.45 and 9.25 m. This suggests that the concentration of fine-grained ferrimagnetic particles in the water-logged layers is too low to affect the observed thermomagnetic behavior. The decrease between 300 °C and 450 °C observed in all samples from subsection I indicates the presence of maghemite which is widely reported in loess-palaeosol samples from the CLP (e.g. Florindo *et al*. 1999; Liu *et al*. 2005; Liu *et al*. 2007a). The rise in the heating curves at about 300 °C for samples from 1.65, 3.75, 5.45, 5.75 and 9.25 m possibly indicates the transformation of weakly magnetic Fe-hydroxides (e.g. lepidocrocite and goethite) to maghemite (Oches & Banerjee 1996; Özdemir & Dunlop 2000). All of the selected samples are characterized by a major decrease near 585 °C, suggesting the presence of nearly stoichiometric magnetite. The gradual decrease from intermediate temperatures to the Curie temperature of magnetite is likely also caused by the transformation of fine-grained particles from single domain to superparamagnetic behavior besides maghemite destruction.

The S-ratio is indicative of the proportion of high coercivity minerals (i.e. hematite and goethite) relative to lower coercivity minerals (i.e. magnetite and maghemite) in the total magnetic mineral assemblage (King & Channell 1991; Verosub & Roberts 1995). The S-ratio values of the Liuwan section (Fig. 5g) range from 0.38

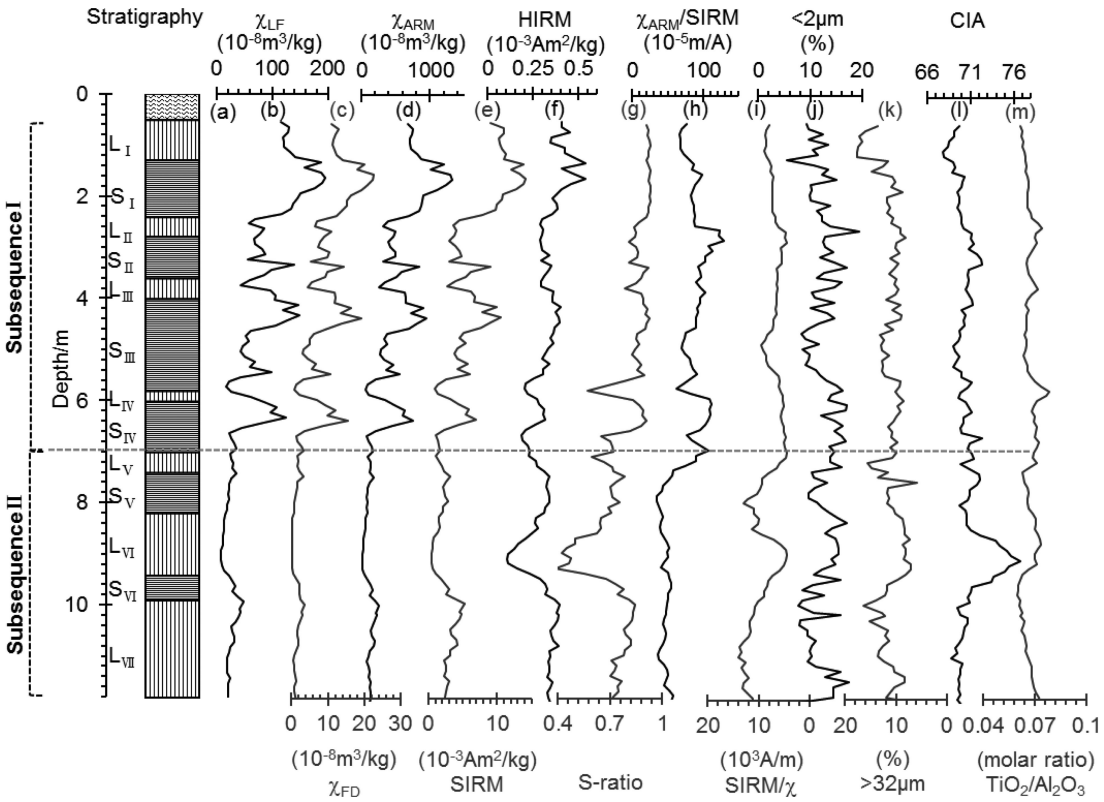


**Figure 5.** Lithology (a), mineral magnetic properties (b–i), per cent sediment grain-size <2 μm and >32 μm, respectively (j, k); Chemical Index of Alteration (l) and $TiO_2/Al_2O_3$ (m) ratio for the Liuwan section.

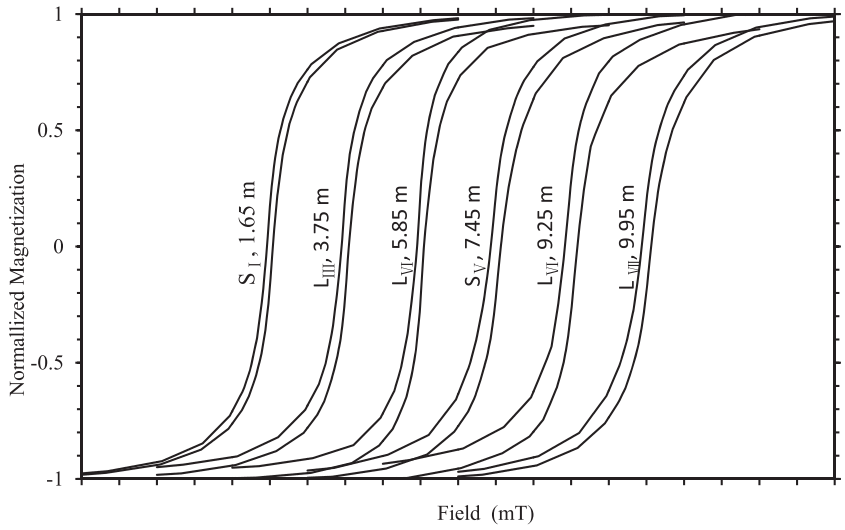


**Figure 6.** Hysteresis loops (after slope correction for the paramagnetic contribution) for selected samples from the Liuwan section. The loops were measured in fields up to ±1.0 T; however, for clarity the maximum field strength plotted is ±500 mT. Each unit of the abscissa axis represents 100 mT.

to 0.94 (mean of 0.80). These values indicate a strong dominance of hematite/goethite over magnetite/maghemite especially in the subsequence II as equal portions of magnetite and hematite will yield an S-ratio of *ca*. 0.98. Further evidence of the presence of imperfect antiferromagnetic minerals is provided by the hysteresis loops (Fig. 6). Almost all the samples exhibit wasp-waisted loops. The open nature of the loops up to fields of 500 mT in the case of samples at 3.75, 5.85, 7.45, 9.25 and 9.95 m, especially in the case of samples with lower S-ratio values in subsequence II, clearly indicates the significant contribution of high-coercivity phases (Deng *et al*. 2004, 2006; Liu *et al*. 2008). These features also support the view that a mixture of both high coercivity and low coercivity components is present in the Liuwan loess deposits (Tauxe *et al*. 1996; Fukuma & Torii 1998; Wang *et al*. 2008).

### 4.2 Magnetic mineral concentration

Subsequence I exhibits higher $\chi$, SIRM and $\chi_{ARM}$ values (Figs 5b,d and e) than subsequence II. Values of $\chi$ range from 16.6–194.6 × $10^{-8}$ $m^3$ $kg^{-1}$ (mean of 95.0 × $10^{-8}$ $m^3$ $kg^{-1}$). Other magnetic

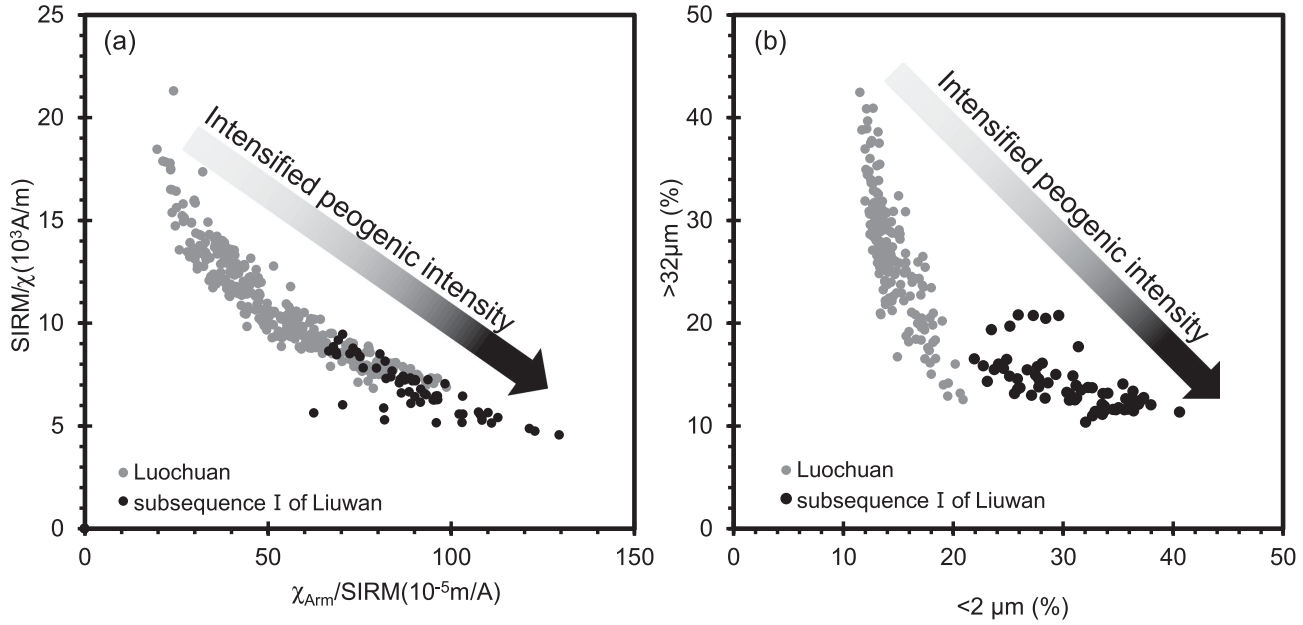


**Figure 7.** Scatter plot of SIRM/$\chi$ and $\chi_{ARM}$/SIRM (a), >32 μm (per cent) and <2 μm (per cent) sediment rain-size fraction (b) for loess samples from the Liuwan section (black circles) and the Luochuan section in the central Chinese Loess Plateau (grey circles).

concentration parameters, that is, SIRM and $\chi_{ARM}$, range from 0.93–14.1 $\times$ $10^{-3}$ $Am^2$ $kg^{-1}$ (mean of 6.98 $\times$ $10^{-3}$ $Am^2$ $kg^{-1}$) and 58.2–1322.0 $\times$ $10^{-8}$ $m^3$ $kg^{-1}$ (mean of 578.6 $\times$ $10^{-8}$ $m^3$ $kg^{-1}$), respectively. These relatively higher $\chi$, SIRM and $\chi_{ARM}$ values, together with the higher S-ratio values, indicate a higher concentration of ferrimagnetic mineral phases in this subsequence. Values of $\chi_{FD}$, which reflects the presence of fine viscous grains close to the SP/SD boundary, range from 0.81–22 $\times$ $10^{-8}$ $m^3$ $kg^{-1}$ (mean of 10.5 $\times$ $10^{-8}$ $m^3$ $kg^{-1}$) (Fig. 5c). Overall these data indicate a higher concentration of magnetite/maghemite in the SP/SD domain state range in Subsequence I.

Compared to lithological subsequence I, the $\chi$, $\chi_{FD}$, $\chi_{ARM}$ and SIRM values of subsequence II exhibit relatively lower values and low-amplitude fluctuations (Figs 5b–e). $\chi$, $\chi_{FD}$, $\chi_{ARM}$ and SIRM range from 8.1–48.6 $\times$ $10^{-8}$ $m^3$ $kg^{-1}$ (mean of 23.6 $\times$ $10^{-8}$ $m^3$ $kg^{-1}$), 0–3.7 $\times$ $10^{-8}$ $m^3$ $kg^{-1}$ (mean of 1.3 $\times$ $10^{-8}$ $m^3$ $kg^{-1}$), 18.4–258.1 $\times$ $10^{-8}$ $m^3$ $kg^{-1}$ (mean of 116 $\times$ $10^{-8}$ $m^3$ $kg^{-1}$) and 0.3–5.2 $\times$ $10^{-3}$ $Am^2$ $kg^{-1}$ (mean of 2.3 $\times$ $10^{-3}$ $Am^2$ $kg^{-1}$), respectively. These data, together with the relatively lower S-ratio values, indicate relatively lower concentrations of both total ferrimagnetic minerals and fine-grained ferrimagnetic components in this subsequence.

HIRM provides a rough estimate of the concentration of imperfect antiferromagnetic minerals (Thompson & Oldfield 1986; King & Channell 1991; Deng *et al*. 2006). Values of HIRM range from 0.2–0.5 $\times$ $10^{-3}$ $Am^2$ $kg^{-1}$ (mean of 0.3 $\times$ $10^{-3}$ $Am^2$ $kg^{-1}$) and 0.1–0.4 $\times$ $10^{-3}$ $Am^2$ $kg^{-1}$ (mean of 0.3 $\times$ $10^{-3}$ $Am^2$ $kg^{-1}$) in subsequences I and II, respectively (Fig. 5f). The small difference in HIRM suggests that the lower S-ratio values of subsequence II are mainly resulted from a lower concentration of ferrimagnetic minerals.

### 4.3 Magnetic grain size

Interparametric ratios such as $\chi_{ARM}$/SIRM and SIRM/$\chi$ can be used to detect variations in ferrimagnetic grain size (Verosub & Roberts 1995; Evans & Heller 2003; Deng *et al*. 2008). Pedogenesis results in the production of fine-grained SP/SD particles while detrital magnetic minerals have a coarser grain size. Alternation in the relative concentration of pedogenic fine-grained SP and SD grains leads to variations in the grain-size distribution of the ferrimagnetic particles (Geiss *et al*. 2004). The ratio SIRM/$\chi$ depends on magnetic grain size and the contribution of SP particles, and it is also affected by paramagnetic phases. $\chi_{ARM}$/SIRM is commonly used as a grain-size indicator of ferrimagnetic minerals, peaking in the SD range and decreasing with increasing grain size (Maher & Taylor 1988); thus $\chi_{ARM}$/SIRM may be a more reliable indicator of ferrimagnetic grain size. Subsequence I exhibits relatively higher $\chi_{ARM}$/SIRM and lower SIRM/$\chi$ ratios (Figs 5h and i) compared to subsequence II. An overall inverse relationship between the two parameters is also confirmed by a cross plot of the two parameters (Fig. 7a), which shows that the samples of subsequence I are enriched in both SP (lower SIRM/$\chi$ due to SP contributions to $\chi$) and SD particles (higher $\chi_{ARM}$/SIRM due to SD contributions to ARM).

### 4.4 Geochemistry and sediment grain-size distribution

The CIA is widely used to evaluate the degree of chemical weathering of terrestrial sediments, with higher CIA values corresponding to higher weathering intensity in the loess deposits of the CLP (Gallet *et al*. 1996, 1998; Yang *et al*. 2006). In the Liuwan section, the CIA range from 67.8–72.3 (mean of 70.1) and 68.7–76.8 (mean of 71.2) in subsequences I and II, respectively (Fig. 5l). These values are higher than those previously reported in the Luochuan section, which range from 62.5–69.5 (mean of 65.5) (Chen *et al*. 2001), suggesting relatively stronger pedogenesis in the Liuwan section.

Al and Ti have the lowest solubility in natural water of all major elements (Sugitani *et al*. 1996). The $TiO_2/Al_2O_3$ ratio is very useful in provenance identification for various sediments (Sheldon & Tabor 2009; Hao *et al*. 2010) because the Ti content may be quite variable among different rock types, even when the Al content remains relatively constant (Li 2000). The $TiO_2/Al_2O_3$ ratio of the Liuwan loess (Fig. 5m) is lower compared to the loess deposits in

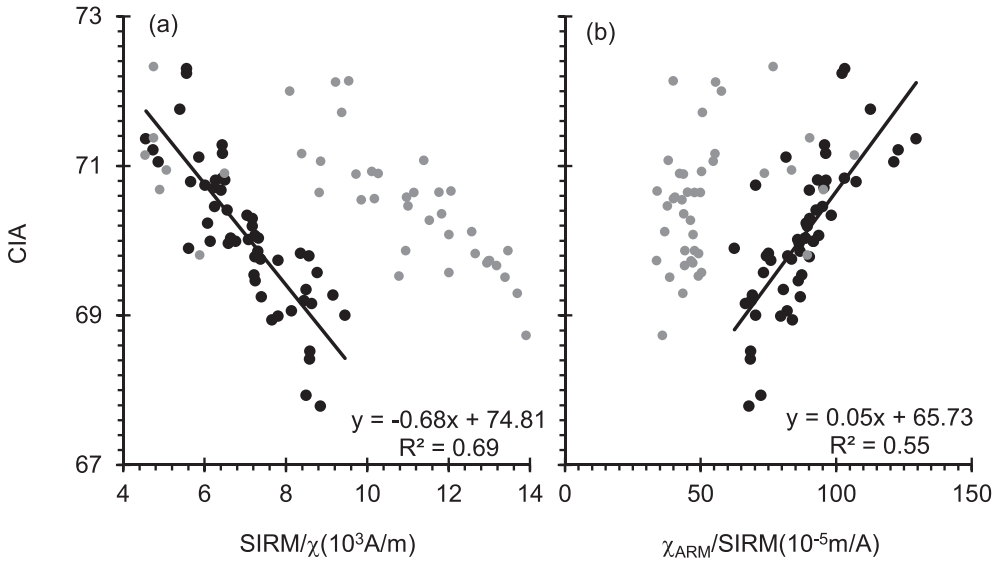


**Figure 8.** Variations of (a) SIRM/$\chi$, (b) $\chi_{ARM}$/SIRM versus CIA for the Liuwan loess deposits. Note that samples from lithological subsequences I (black circles) and II (grey circles) of the section fall into two distinct groups.

south China (Li *et al*. 1999; Hao *et al*. 2012) and higher compared to the loess deposits of the CLP (Gallet *et al*. 1996; Liang *et al*. 2009).

Grain-size variations of loess-palaeosol sequences on the CLP are indicators of the transport capacity of the winds, and the depositional environment (Ding *et al*. 1994; Porter *et al*. 2001). The fine fraction exhibits a roughly similar pattern of variation to the CIA, and the coarse fraction exhibits an inverse pattern to the CIA (Figs 5j,k and l). Both fine and coarse fractions exhibit lower amplitudes of variation compared to the CLP (Porter & An 1995; Liu & Ding 1998; Liu *et al*. 1999a).

## 5 DISCUSSION

### 5.1 Role of water-logging for the magnetic properties of lithological subsequence II

The sediments of subsequence II are similar to subsequence I with regard to bulk grain-size distribution and REE distribution (Zhang *et al*. 2012). However, our results indicate that the values of $\chi$, SIRM, $\chi_{FD}$ and $\chi_{ARM}$ of subsequence II (7–11.8 m), are low and uniform compared to subsequence I. There are two possible explanations for this finding: (1) change of the eolian composition due to a different source; and (2) post-depositional dissolution or transformation of ferrimagnetic phases.

The parent material of the loess deposits of the Luonan basin is derived from two sources: one source is the local clastic deposits produced from the weathered bedrock of the proximal orogenic belt and adjacent alluvial/fluvial sediments; the other source is from the deserts, piedmont alluvial fans and dryland areas in northern and northwestern China (Zhang *et al*. 2012). However, we argue that the fluctuation in the relative input of the two sources of parent material is an unlikely explanation for two reasons. First, the $TiO_2/Al_2O_3$ ratio, which is widely used in provenance identification for various sediments, exhibits no abrupt shift between subsequence I and II. Second, Sr-Nd isotopic composition, long considered as a useful indicator of dust provenance, also suggests that the parent material of the subsequences I and II is homogeneous (Zhang *et al*. 2012).

With regard to dissolution or transformation of ferrimagnetic phases, the presence of olive yellow (5GY 8/3) aggregates in subsequence II, found by field investigation, provides strong evidence of water-logging and the occurrence of redoxomorphic processes. The post-depositional alteration of magnetic properties associated with water-logging has been reported in loess deposits in Alaska (Liu *et al*. 2001), Argentina (Orgeira *et al*. 2003.), Siberia (Matasova *et al*. 2001), Germany (Terhorst *et al*. 2001; Baumgart *et al*. 2013; Taylor *et al*. 2014) and also in the southern CLP (Guo *et al*. 2013). $Fe^{3+}$ is reduced to $Fe^{2+}$ under anoxic conditions, and soluble $Fe^{2+}$, upon the return of oxic conditions, would be available for *in situ* mineralization of new iron oxides, favouring the formation of $Fe^{3+}$ oxides and oxyhydroxides (Liu *et al*. 1999b; Taylor *et al*. 2014). It is postulated that fine-grained magnetite/maghemite is preferentially removed with respect to the coarser grains in water-saturated zones that are subjected to reducing conditions, leading to coarser-grained magnetic mineral signatures in parts of the altered horizons. More intensive and prolonged dissolution may gradually reduce the grain size of the remaining coarse-grained magnetic phases (Ao *et al*. 2010; Taylor *et al*. 2014). The results would be a reduction in the concentration of ferrimagnetic particles, depletion of the fine-grained fraction including superparamagnetic grains, and an increase in the magnetic 'hardness' of the altered horizon.

Figs 8(a) and (b) illustrate plots of SIRM/$\chi$ and $\chi_{ARM}$/SIRM versus the CIA (i.e. pedogenic intensity). The samples from subsequence II exhibit significantly higher values of SIRM/$\chi$ and lower values of $\chi_{ARM}$/SIRM than those from subsequence I with respect to similar values of CIA. The relatively higher SIRM/$\chi$ ratios of subsequence II can be attributed to the relatively lower $\chi$ values due to loss of SP particles and the relatively lower $\chi_{ARM}$/SIRM ratios can be attributed to relatively lower $\chi_{ARM}$ values due to loss of SD magnetic particles in reduction conditions. The increased magnetic 'hardness' (Fig. 5g) also suggests the dissolution of ferrimagnetic particles in subsequence II, enhancing the relative contribution of hematite and goethite. All of the aforementioned evidence indicates alteration induced by water-logging as the primary control of the observed magnetic properties in subsequence II.

### 5.2 Palaeoclimate proxies and pedogenic overprinting

Detailed magnetic studies of the loess-palaeosol sequences on the CLP suggest that pedogenic processes may favour the formation of SP/SD magnetite/maghemite (Banerjee & Hant 1993; Liu *et al*. 2007a). Warmer and wetter interglacial periods promoted intensive pedogenesis and formation of higher volume of ferrimagnetic (FM) particles in the soils (Zhou *et al*. 1990; Maher & Thompson 1999). Our rock-magnetic investigation indicate that the palaeosol layers in subsection I of the studied section exhibit higher values of both $\chi$ and $\chi_{FD}$ with respect to the intervening loess layers (Figs 3b and 5b,c). It seems that pedogenesis, which is well documented in the CLP (Zhou *et al*. 1990; Maher 1998; Deng *et al*. 2004; Liu *et al*. 2007a), also plays an important role in driving the variations of the magnetic properties in subsequence I of the Liuwan loess section.

Magnetic-concentration-related parameters such as $\chi$ are significantly affected by the soil parent material which limits their application in large-scale regions (Blundell *et al*. 2009). If the modern atmospheric circulation patterns remained the same during the past 600 ka (Hao & Guo 2005), the Liuwan section, located at the warmer and wetter end of a NW-SE gradient of summer monsoon climate (Fig. 1), should have higher $\chi$ values, based on the precipitation and susceptibility patterns observed on the CLP. The maximum $\chi$ values of the Liuwan section ($194.6 \times 10^{-8}$ m$^3$ kg$^{-1}$), Shangbaichuan section ($161.7 \times 10^{-8}$ m$^3$ kg$^{-1}$) (Zhao *et al*. 2008) and Shangzhou section ($130 \times 10^{-8}$ m$^3$ kg$^{-1}$; Lei 1999) in the study area are lower than those for Luochuan ($259 \times 10^{-8}$ m$^3$ kg$^{-1}$) and Duanjiapo ($344 \times 10^{-8}$ m$^3$ kg$^{-1}$) in the central and southern CLP (Bloemendal & Liu 2005; Bloemendal *et al*. 2008). The existence of multiple sediment sources may be problematic for the application of transfer functions developed from the CLP to palaeoclimatic reconstruction in the study area. Thus, the use of magnetic properties as a proxy for reconstructing palaeoprecipitation in the area is tenuous.

Pedogenesis results in the production of fine-grained SP/SD particles while detrital magnetic minerals have a coarser grain size (Liu *et al*. 2007b). Changes in the relative concentration of pedogenic fine-grained SP and SD grains leads to variations in the grain-size distribution of the ferrimagnetic particles (Geiss *et al*. 2004). The original $\chi_{ARM}$/SIRM value of the loess parent material is modulated by the pedogenic SD particles and thus $\chi_{ARM}$/SIRM can be used as a palaeoclimate proxy if the pedogenic magnetic minerals are similar throughout the study region (Geiss *et al*. 2008). In subsequence I, $\chi_{ARM}$/SIRM is positively correlated with the CIA ($r^2 = 0.55$) due to the pedogenic SD fraction and SIRM/$\chi$ is negatively correlated with the CIA ($r^{22} = 0.69$) due to the pedogenic SP fraction having a high $\chi$ value (Fig. 8). Thus the magnetic ratios can be linked to weathering intensity which reflects climate conditions.

Caution is also needed in using grain-size-related parameters as proxies to reconstruct palaeoclimate in the loess layers in the study area. The winter monsoon brought more aeolian dust into the CLP, resulting in a higher sediment accumulation rate and thicker loess/palaeosol layers (Ding *et al*. 1994; Liu & Ding 1998). At the Luochuan section in the central CLP, the thickness from L1 to S5 is 40.6 m (Kukla *et al*. 1988); in contrast, the thickness of the same interval at Liuwan section, assuming that the stratigraphic correlation in Fig. 3 is credible, is only 7.0 m. This indicates that the sediment accumulation rate was significantly lower, especially during interglacial periods with a weakened winter monsoon. Fine-grained magnetic particles will likely also affect a large portion of the underlying glacial sediments (loess layers) where interglacial sediments (palaeosol layers) are relatively thin and insufficiently thick to isolate the underlying loess from the effects of pedogenesis that is active on the new land surface. The fine-grained magnetic particles of pedogenic origin formed during subsequent interglacial periods in the underlying loess layer would lead to lower SIRM/$\chi$ and higher $\chi_{ARM}$/SIRM ratios with respect to the initial state formed in the glacial period, thus tending to erase the signal of the cold, dry climatic phases. What is more, it is suggested that not only the entire loess layer but also the previous formed palaeosol layer below may be afftected by pedogenic overprinting considering the thin loess layers in subsequence I (Table 1, Fig. 2).

### 5.3 Palaeoenvironmental implications for early humans

The rock-magnetic and field investigations resulted in the division of the Liuwan sequences into two subsequences: subsequence I, with higher values and fluctuations of magnetic concentration parameters; and subsequence II, characterized by low and uniform values of magnetic concentration parameters and olive yellow (5GY 8/3) aggregates indicating water-logging and redoxomorphic processes. Similar cases are also reported at Shangbaichuan (Zhao *et al*. 2008), and Qiaojiayao (Lu *et al*. 2011a) in the study area. Overall, the magnetic, grain-size and geochemical records reflect major aspects of the palaeoenvironment of the area.

The eastern Qingling Mountains experienced a phased uplift process since the middle Pleistocene, forming a series of river terraces (Xue *et al*. 2004; Pang *et al*. 2015). The loess deposits in the Liuwan sequences began to accumulate on the flood plain after the tectonic uplift which formed the terrace underlying subsequence II. However, sediment accumulation and ongoing pedogenic processes were frequently affected by flooding. Temporary water-saturated conditions related to flooding may have caused the destruction of fine-grained magnetic particles and increased the magnetic 'hardness', as discussed in Section 5.1. This process continued during two glacial/interglacial cycles ($L_{VII}$, $S_{VI}$, $L_{VI}$, $S_V$, $L_V$) and became less frequent till the formation of the base of subsequence I ($L_V$, $S_{VI}$).

The stagnic and gleyic features disappear in the upper loess deposits due to aggradation and/or progressing uplift of the Qingling Mountains, and thus neoformation of magnetic minerals began to play an important role in driving the variations of the magnetic properties in subsequence I. As discussed in Section 5.2, the SIRM/$\chi$ and $\chi_{ARM}$/SIRM values may reflect weathering intensity and therefore climate conditions in subsequence I. However, pedogenic overprinting may be a significant problem for climatic reconstruction within the loess layers. The coarse-grained sediment fraction can be used as a proxy index of East Asian winter monsoon strength, while the fine fraction reflects pedogenesis (Liu & Ding 1998; Lu & An 1998). The lower percentage of the coarse fraction (>32 μm) content and the higher percentage of the fine fraction (<2 μm) content, and the higher CIA values, indicate warmer and more humid interglacials in the study area compared to Luochuan in the central CLP (Fig. 7b). $C_3$ (woody) plants may have dominated the vegetation which consisted of a mixture $C_3$ and $C_4$ plants (grasses), as suggested by carbon isotope results (Zhang *et al*. 2009). In addition, it may be significant that Palaeolithic stone artefacts have been discovered in both loess and palaeosol horizons, suggesting that an environment favourable for humans occurred during both glacials and interglacials. The SIRM/$\chi$ and $\chi_{ARM}$/SIRM values of the Liuwan section compared with those from the Luochuan section (Fig. 7a) obviously well represent these warmer and more humid

climate conditions, most likely better than the magnetic concentration values.

## 6 CONCLUSIONS

Loess/palaeosol sequences from the Eastern Qingling Mountains provide a suitable archive for the study of the environment of early humans. The results of rock magnetic, geochemical and grain-size measurements of the Liuwan loess sequences lead to following conclusions:

(1) The magnetic mineral assemblage is composed of magnetite/maghemite and hematite/goethite. Magnetite/maghemite makes a major contribution to the magnetic properties in subsequence I, whereas the S-ratio indicates a strong dominance of hematite/goethite over magnetite/maghemite in subsequence II.

(2) The weak magnetic properties of subsequence II are associated with waterlogging-induced redoxomorphic processes. Subsequent to the formation of the underlying terrace, flooding may have played an important role in determining the magnetic properties of this subsequence.

(3) Magnetic susceptibility is widely used as a proxy for palaeoprecipitation in the CLP; however, we suggest that it is not appropriate to use it in the study area. The interparametric ratios such as SIRM/$\chi$ and $\chi_{ARM}$/SIRM are potentially better indicators of palaeoclimate, and we surmise that the values and amplitude of variation of these ratios, together with the bulk grain-size and CIA values, point to a relatively warm, humid interglacial period which was more favourable for early man than coeval environments of the CLP.

## ACKNOWLEDGEMENTS

We sincerely thank the following: J. Bloemendal for providing magnetic data of the Luochuan sections; and F. Oldfield, Qingsong Liu, Xianyan Wang, Xusheng Li, Shuangwen Yi, Xuefeng Sun and Limin Zhou for their valuable suggestions. We also wish to thank Erwin Appel, Christoph E. Geiss and Eduard Petrovsky (the associate Editor) for their helpful and constructive comments. This study was supported by the National Natural Science Foundation of China (41272187 and 40802036), China National Science and Technology Basic Work Program (2012FY111700) and the State Key R&D Project of China (2016YFA0600500).

## REFERENCES

An, Z., 2000. The history and variability of the East Asian paleomonsoon climate, *Quat. Sci. Rev.,* **19,** 171–187.

Ao, H., Deng, C., Dekkers, M.J. & Liu, Q., 2010. Magnetic mineral dissolution in Pleistocene fluvio-lacustrine sediments, Nihewan Basin (North China), *Earth planet. Sci. Lett.,* **292,** 191–200.

Banerjee, S.K. & Hant, C.P., 1993. Separation of local signals from the regional paleomonsoon record of the Chinese Loess Plateau: a rock-magnetic approach, *Geophys. Res. Lett.,* **20,** 843–846.

Baumgart, P., Hambach, U., Meszner, S. & Faust, D., 2013. An environmental magnetic fingerprint of periglacial loess: records of Late Pleistocene loess-palaeosol sequences from Eastern Germany, *Quat. Int.,* **296,** 82–93.

Bloemendal, J. & Liu, X., 2005. Rock magnetism and geochemistry of two plio-pleistocene Chinese loess-paleosol sequences-implications for quatitative paleoprecipitation reconstruction, *Palaeogeogr. Palaeoclimatol. Palaeoecol.,* **226,** 149–166.

Bloemendal, J., King, J.W., Hall, F.R. & Doh, S.J., 1992. Rock magnetism of late Neogene and Pleistocene deep-sea sediments: relationship to sediment source, diagenetic processes, and sediment lithology, *J. geophys. Res.,* **97,** 4361–4375.

Bloemendal, J., Liu, X., Sun, Y. & Li, N., 2008. An assessment of magnetic and geochemical indicators of weathering and pedogenesis at two contrasting sites on the Chinese Loess plateau, *Palaeogeogr. Palaeoclimatol. Palaeoecol.,* **257,** 152–168.

Blundell, A., Dearing, J.A., Boyle, J.F. & Hannam, J.A., 2009. Controlling factors for the spatial variability of soil magnetic susceptibility across England and Wales, *Earth-Sci. Rev.,* **95,** 158–188.

Chen, J., An, Z., Liu, L., Junfeng, J., Yang, J. & Chen, Y., 2001. Variations in chemical compositions of the eolian dust in Chinese Loess Plateau over the past 2.5 Ma and chemical weathering in the Asian inland, *Sci. China (Earth Sci.),* **44,** 403–413.

Deng, C., Zhu, R., Verosub, K.L., Singer, M.J. & Vidic, N.J., 2004. Mineral magnetic properties of loess/paleosol couplets of the central loess plateau of China over the last 1.2 Myr, *J. geophys. Res.,* **109,** B01103, doi:10.1029/2003JB002532.

Deng, C., Shaw, J., Liu, Q., Pan, Y. & Zhu, R., 2006. Mineral magnetic variation of the Jingbian loess/paleosol sequence in the northen Loess Plateau of China: implications for Quaternary development of Asian aridification and cooling, *Earth planet. Sci. Lett.,* **241,** 248–259.

Deng, C., Zhu, R., Ao, H. & Pan, Y., 2008. Timing of the Nihewan formation and faunas, *Quat. Res.,* **69,** 77–90.

Ding, Z., Yu, Z., Rutter, N.W. & Liu, T., 1994. Towards an orbital time scale for chinese loess deposits, *Quat. Sci. Rev.,* **13,** 39–70.

Dunlop, D.J. & Özdemir, Ö., 1997. *Rock Magnetism: Fundamentals and Frontiers*, Cambridge Univ. Press.

Evans, M.E. & Heller, F., 2003. *Environmental Magnetism:Principles and Applications of Enviromagnetics*, Academic Press.

Florindo, F., Zhu, R., Guo, B., Yue, L., Pan, Y. & Speranza, F., 1999. Magnetic proxy climate results from the Duanjiapo loess section, southernmost extremity of the Chinese loess Plateau, *J. geophys. Res.,* **104,** 645–659.

Fukuma, K. & Torii, M., 1998. Variable shape of magnetic hysteresis loops in the Chinese loess-paleosol sequence, *Earth Planets Space,* **50,** 9–14.

Gallet, S., Jahn, B.-m. & Torii, M., 1996. Geochemical characterization of the Luochuan loess-paleosol sequence, China, and paeloclimatic implications, *Chem. Geol.,* **133,** 67–88.

Gallet, S., Jahn, B.-m., Lanoë, B.V.V., Aline, Dia & Rossello, E., 1998. Loess geochemistry and its implications for particle origin and composition of the upper continental crust, *Earth planet. Sci. Lett.,* **156,** 157–172.

Geiss, C.E., Zanner, C.W., Banerjee, S.K. & Joanna, M., 2004. Signature of magnetic enhancement in a loessic soil in Nebraska, United States of America, *Earth planet. Sci. Lett.,* **228,** 355–367.

Geiss, C.E., Egli, R. & Zanner, C.W., 2008. Direct estimates of pedogenic magnetite as a tool to reconstruct past climates from buried soils, *J. geophys. Res.,* **113,** B11102, doi:10.1029/2008JB005669.

Guo, X., Liu, X., Li, P., Lü, B., Guo, H., Chen, Q., Liu, Z. & Ma, M., 2013. The magnetic mechanism of paleosol S5 in the Baoji section of the southern Chinese Loess Plateau, *Quat. Int.,* **306,** 129–136.

Hao, Q. & Guo, Z., 2005. Spatial variations of magnetic susceptibility of Chinese loess for the last 600 kyr: implications for monsoon evolution, *J. geophys. Res.,* **110,** B12101, doi:10.1029/2005JB003765.

Hao, Q., Guo, Z., Qiao, Y., Xu, B. & Oldfield, F., 2010. Geochemical evidence for the provenance of middle Pleistocene loess deposits in southern China, *Quat. Sci. Rev.,* **29,** 3317–3326.

Hao, Q. *et al.*, 2012. Delayed build-up of Arctic ice sheets during 400, 000-year minima in insolation variability, *Nature,* **490,** 393–396.

Heller, F. & Liu, T., 1982. Magnetostratigraphical dating of loess deposits in China, *Nature,* **300,** 431–433.

Hu, X.F., Wei, J., Xu, L.-F., Zhang, G.-L. & Zhang, W.-G., 2009. Magnetic susceptibility of the Quaternary Red Clay in subtropical China and its paleoenvironmental implications, *Palaeogeogr. Palaeoclimatol. Palaeoecol.,* **279,** 216–232.

Hunt, C.P., Banerjee, S.K., Han, J.M., Solheid, P.A., Oches, E.A., Sun, W. & Liu, T., 1995. Rock-magnetic proxies of climate change in the loess-paleosol sequences of the western Loess Plateau of China, *Geophys. J. Int.,* **123,** 232–244.

King, J.W. & Channell, J.E.T., 1991. Sedimentary magnetism, environmental magnetism, and magnetostratigraphy, US National Report to IUGG, *Rev. Geophys.,* **29,** 358–370.

Kukla, G., Heller, F., Liu, X.M., Xu, T.C., Liu, T.S. & An, Z.S., 1988. Pleistocene climates in China dated by magnetic susceptibility, *Geology,* **16,** 811–814.

Lei, X., 1999. Paleoenvironmental changes recorded by Shangzhou loess-paleosol sequences on the eastern Qinling Mts during the last 0.6Ma, *Mar. Geol. Quat. Geol.,* **19,** 63–73 (in Chinese with English abstract).

Li, Y.H., 2000. *A Compendium of Geochemistry: From Solar Nebula to the Human Brain*, Princeton Univ. Press.

Li, X. & Yang, D., 1999. OXide-Geochemistry features and paleoclimatic record of the aeolian-dust depositional sequence in Southern Anhui, *Mar. Geol. Quat. Geol.,* **19,** 75–82 (in Chinese with English abstract).

Li, X.S., Yang, D.Y. & Lu, H.Y., 1999. Oxide-geochemistry features and paleoclimatic record of the aeolian-dust depositional sequence in southern Anhui., *Mar. Geol. Quat. Geol.,* **19,** 75–82 (in Chinese with English abstract).

Liang, M., Guo, Z., Kahmann, A.J. & Oldfield, F., 2009. Geochemical characteristics of the Miocene eolian deposits in China: their provenance and climate implications, *Geochem. Geophys. Geosyst.,* **10,** Q04004, doi:10.1029/2008GC002331.

Liu, T.S. & Ding, Z.L., 1998. Chinese loess and the paleomonsoon, *Ann. Rev. Earth Planet. Sci.,* **26,** 111–145.

Liu, Q., Deng, C., Yu, Y., Torrent, J., Jackson, M.J., Banerjee, S.K. & Zhu, R., 2005. Temperature dependence of magnetic susceptibility in an argon environment: implications for pedogenesis of Chinese loess/palaeosols, *Geophys. J. Int.,* **161,** 102–112.

Liu, Q., Deng, C., Torrent, J. & Zhu, R., 2007a. Review of recent developments in mineral magnetism of the Chinese loess, *Quat. Sci. Rev.,* **26,** 368–383.

Liu, Q., Roberts, A.P., Torrent, J., Horng, C.-S. & Larrasoaña, J.C., 2007b. What do the HIRM and S-ratio really measure in environmental magnetism? *Geochem. Geophys. Geosyst.,* **8,** Q09011, doi:10.1029/2007GC001717.

Liu, C., Xu, X., Yuan, B. & Deng, C., 2008. Magnetostratigraphy of the Qiliting section (SE China) and its implication for geochronology of the red soil sequences in southern China, *Geophys. J. Int.,* **174,** 107–117.

Liu, T., Ding, Z. & Rutter, N., 1999a. Comparison of Milankovitch periods between continental loess and deep sea records over the last 2.5 Ma, *Quat. Sci. Rev.,* **18,** 1205–1212.

Liu, X.M., Hesse, P., Rolph, T. & Begét, J.E., 1999b. Properties of magnetic mineralogy of Alaskan loess: evidence for pedogenesis, *Quat. Int.,* **62,** 93–102.

Liu, X.M., Hesse, P., Begét, J. & Rolph, T., 2001. Pedogenic destruction of ferrimagnetics in Alaskan loess deposits, *Aust. J. Soil Res.,* **39,** 99–115.

Lu, H. & An, Z., 1998. Paleoclimatic significance of grain size of loess-palaeosol deposit in Chinese Loess Plateau, *Sci. China D,* **41,** 626–631.

Lu, H., Zhang, H., Wang, S., Cosgrove, R., Zhao, C., Stevens, T. & Zhao, J., 2007. A preliminary survey on loess deposit in eastern Qinling Mountains (central China) and its implication for estimating age of the Pleistocene lithic artifacts, *Quat. Sci.,* **27,** 559–567 (in Chinese with English abstract).

Lu, H., Sun, X., Wang, S., Cosgrove, R., Zhang, H., Yi, S., Ma, X., Wei, M. & Yang, Z., 2011a. Ages for hominin occupation in Lushi Basin, middle of South Luo River, central China, *J. Human Evol.,* **76,** 142–147.

Lu, H., Zhang, H., Wang, S., Cosgrove, R., Sun, X., Zhao, J., Sun, D., Zhao, C., Shen, C. & Wei, M., 2011b. Multiphase timing of hominin occupations and the paleoenvironment in Luonan Basin, Central China, *Quat. Res.,* **76,** 142–147.

Maher, B.A., 1998. Magnetic properties of modern soils and Quaternary loessic paleosols: paleoclimatic implications, *Palaeogeogr. Palaeoclimatol. Palaeoecol.,* **137,** 25–54.

Maher, B.A. & Taylor, R., 1988. Formation of ultrafine-grained magnetite in soils, *Nature,* **336,** 368–370.

Maher, B.A. & Hu, M., 2006. A high-resolution record of Holocene rainfall variations from the western Chinese Loess Plateau: antiphase behaviour of the African/Indian and East Asian summer monsoons, *Holocene,* **16,** 309–319.

Maher, B.A. & Thompson, R., 1999. Paleoclimatic significance of the mineral magnetic record of Chinese loess and paleosols, *Quat. Res.,* **37,** 155–170.

Matasova, G., Petrovský, E., Jordanova, N., Zykina, V. & Kapička, A., 2001. Magnetic study of Late Pleistocene loess/palaeosol sections from Siberia: palaeoenvironmental implications, *Geophys. J. Int.,* **147,** 367–380.

Nesbitt, H.W. & Young, G.M., 1982. Early Proterozoic climates and plate motions inferred from major element chemistry of lutites, *Nature,* **299,** 715–717.

Norton, C.J. & Bae, K., 2008. The Movius Line sensu lato (Norton *et al*. 2006) further assessed and defined, *J. Human Evol.,* **55,** 1148–1150.

Oches, E.A. & Banerjee, K., 1996. Rock-magnetic proxies of climate change from loess-paleosol sediments of the Czech Republic, *Stud. Geophys. Geod.,* **40,** 287–300.

Orgeira, M.J., Walther, A.M., Tó falo, R.O., Vásquez, C., Berquó, T., Favier Dobois, C. & Bohnel, H., 2003. Environmental magnetism in fluvial and loessic Holocene sediments and paleosols from the Champean plain (Argentina), *J. South Am. Earth Sci.,* **16,** 259–274.

Özdemir, Ö. & Dunlop, D.J., 2000. Intermediate magnetite formation during dehydration of goethite, *Earth planet. Sci. Lett.,* **177,** 59–67.

Pang, J., Chunchang, H., Yali, Z., Xiaochun, Zha, Yuzhu, Z. & Leibin, W., 2015. Eolian loess-palaeosol sequence and OSL age of the first terraces within the Yunxian Basin along the upper Hanjiang River, *Acta Anthropolgica Sin.,* **70,** 63–72 (in Chinese with English abstract).

Porter, S.C. & An, Z., 1995. Correlation between climate events in the North Atlantic and China during the last glaciation, *Nature,* **375,** 305–308.

Porter, S.C., Singhvi, A., An, Z. & Lai, Z., 2001. Luminescence age and palaeoenvironmental implications of a late Pleistocene ground wedge on the Northeastern Tibetan Plateau, *Permafrost Periglac. Process.,* **12,** 203–210.

Qiao, Y. *et al.*, 2003. Loess-soil sequences in southern Anhui Province: magnetostratigraphy and paleoclimatic significance, *Chin. Sci. Bull.,* **48,** 2088–2093.

Robinson, S.G., 1986. The late Pleistocene palaeoclimatic record of North Atlantic deep-sea sediments revealed by mineral-magnetic measurements, *Phys. Earth planet. Inter.,* **42,** 22–47.

Shaanxi Provincial Institute of Archaeology Cultural Relics Administrative Committee of Shangluo District, M.o.L.C., 2007. *Huashilang (I): The Paleolithic Open-air Sites in the Luonan Basin, China*, Science Press.

Sheldon, N.D. & Tabor, N.J., 2009. Quantitative paleoenvironmental and paleoclimatic reconstruction using paleosols, *Earth-Sci. Rev.,* **95,** 1–52.

Sugitani, K., Horiuchi, Y., Adachi, M. & Sugisaki, R., 1996. Anomalously low $Al_2O_3/TiO_2$ values for Archean cherts from the Pilbara Block, Western Australia-possible evidence for extensive chemical weathering on the early earth, *Precambrian Res.,* **80,** 49–76.

Tauxe, L., Mullender, T.A.T. & Pick, T., 1996. Potbellies, wasp-waists, and superparamagnetism in magnetic hysteresis, *J. geophys. Res.,* **101,** 571–583.

Taylor, S.N., Lagroix, F., Rousseau, D.-D. & Antoine, P., 2014. Mineral magnetic characterization of the Upper Pleniglacial Nussloch loess sequence (Germany): an insight into local environmental processes, *Geophys. J. Int.,* **199,** 1463–1480.

Terhorst, B., Appel, E. & Werner, A., 2001. Palaeopedology and magnetic susceptibility of a loess-palaeosol sequence in southwest Germany, *Quat. Int.,* **76,** 231–240.

Thompson, R. & Oldfield, F., 1986. *Environmental Magnetism*, Allen and Unwin.

Verosub, K.L. & Roberts, A.P., 1995. Environmental magnetism: past, present, and future, *J. geophys. Res.,* **100**(B2), 2175–2192.

Wang, S., 2005. *Perspectives on Hominid Behaviour and Settlement Patterns: A Study of the Lower Paleolithic Sites in the Luonan Basin, China*, British Archaeological Reports.

Wang, S., Shen, C., Hu, S., Zhang, X., Wang, C. & Cosgrove, R., 2005. Lithic artefacts collected from open-air sites during 1995–1999. Investigations in Luonan Basin, China, *Acta Anthropolgica Sin.,* **24,** 87–103 (in Chinese with English abstract).

Wang, X., Løvlie, R., Su, P. & Fan, X., 2008. Magnetic signature of environmental change reflected by Pleistocene lacustrine sediments from the

Nihewan Basin, North China, *Palaeogeogr. Palaeoclimatol. Palaeoecol.,* **260,** 452–462.

Xue, X., Li, H., Li, Y. & Liu, H., 2004. The new data of the uplifting of Qinling Mountains sice the middle Pleistocene, *Quat. Sci.,* **24,** 82–87 (in Chinese with English abstract).

Yang, S.L., Ding, F. & Ding, Z.L., 2006. Pleistocene chemical weathering history of Asian arid and semi-arid regions recorded in loess deposits of China and Tajikistan, *Geochim. Cosmochim. Acta,* **70,** 1695–1709.

Yang, J., Li, G., Rao, W. & Ji, J., 2009. Isotopic evidences for provenance of East Asian Dust, *Atmos. Environ.,* **43,** 4481–4490.

Zhang, H., Lu, H., Jiang, S.-Y., Vandenberghe, J., Wang, S. & Cosgrove, R., 2012. Provenance of loess deposits in the Eastern Qinling Mountains (central China) and their implications for the paleoenvironment, *Quat. Sci. Rev.,* **43,** 94–102.

Zhang, P., Liu, W., Lu, H., Zhou, W. & Zhao, C., 2009. Organic carbon isotope composition of Luonan loess compared with that of Luochuan and Xifeng loess, *Quat. Sci.,* **29,** 34–42 (in Chinese with English abstract).

Zhang, W., Yu, L., Lu, M., Zheng, X. & Shi, Y., 2007. Magnetic properties and geochemistry of the Xiashu Loess in the present subtropical area of China, and their implications for pedogenic intensity, *Earth planet. Sci. Lett.,* **260,** 86–97.

Zhao, J., Lu, H., Wang, X., Zhang, H. & Wang, S., 2008. Magnetic properties of loess deposit in Eastern Qinling Moutains and an investigation on the magnetic susceptibility enhancement, *Acta Seismol. Sin.,* **26,** 1052–1062.

Zheng, X., 1999. *Eolian Deposition and Environment in Changjiang Delta and Exitending Sea Areas*, East China Normal University Press.

Zhou, L.P., Oldfield, F., Wintle, A.G., Robinson, S.G. & Wang, J.T., 1990. Partly pedogenic origin of magnetic variations in Chinese loess, *Nature,* **346,** 737–739.

Zhu, R., An, Z., Pott, R. & Hoffman, K.A., 2003. Magnetostratigraphic dating of early humans in China, *Earth-Sci. Rev.,* **61,** 341–359.